Advanced Laser Vibrometry in Pulsed Mode using Poly-Pulse Waveforms and Time-frequency Processing

Julien Totems, Véronique Jolivet, Jean-Philippe Ovarlez, Nadine Martin

▶ To cite this version:

HAL Id: hal-00556221

https://hal.archives-ouvertes.fr/hal-00556221v2

Submitted on 5 Feb 2010

ADVANCED LASER VIBROMETRY IN PULSED MODE USING POLY-PULSE WAVEFORMS AND TIME-FREQUENCY PROCESSING

Julien Totems [1], Véronique Jolivet [1], Jean-Philippe Ovarlez [1], Nadine Martin [2]

[1] Onera The French Aerospace Lab, Chemin de la Hunière, 91761 Palaiseau Cedex, France - Email: julien.totems@onera.fr

[2] Gipsa-Lab, 961 rue de la Houille Blanche, Domaine Universitaire BP 46, F-38402 Saint-Martin d'Hères, France - Email: nadine.martin@gipsa-lab.inpg.fr

ABSTRACT

Vibration sensing by laser radar with a pulsed emission is a promising technique for long range target recognition and identification. However, compared to its continuous-wave counterpart, it is impaired by its greater sensitivity to speckle noise and its lack of robustness to multiple independent vibrations of the target surface. Using poly-pulse waveforms for greater velocity resolution, we developed a new estimator to take into account signal statistics, and time frequency representations that can achieve better performance than classical processing methods. Simulations show a 5dB improvement in Signal-to-Noise Ratio (SNR) when speckle noise is dominant, and 4dB improvement when signal is weak in regard to detection noise.

1. INTRODUCTION

Because of their great velocity sensitivity, coherent laser radars (ladars) are able to sense micrometric vibrations of remote or inaccessible targets. This capability has been used for civilian applications, such as structural diagnosis of potentially damaged buildings [1], and for military applications by using vibrational features for target recognition and identification at ranges beyond the reach of conventional imaging systems [2,3].

All-fiber vibrometers are today the most compact and easy to build, many fibered components being available for telecommunications wavelength 1.55µm. The layout and principle of a fiber laser vibrometer is summarized on Fig. 1. The goal is to measure the Doppler frequency modulation induced by the target vibration velocity on the backscattered laser wave. Coherent heterodyne detection is performed by mixing the received optical wave with part of the emission (local oscillator). Their interference is the source of a heterodyne signal at the output of a detector. Signal processing first aims to recover the velocity time series of the target, by estimating the Instantaneous Frequency (IF) of the signal: $f_{inst}(t) = f_{AOM} + 2v(t)/\lambda$, with λ the laser wavelength.

Then, by taking the Fourier Tranform (FT) of the vibrational velocity, a vibration spectrum is obtained. Commonly exploited features include the modal and engine vibration frequencies of the target, which create identifiable peaks on the spectrum. Matching these features with a database allows the identification of the target [2].
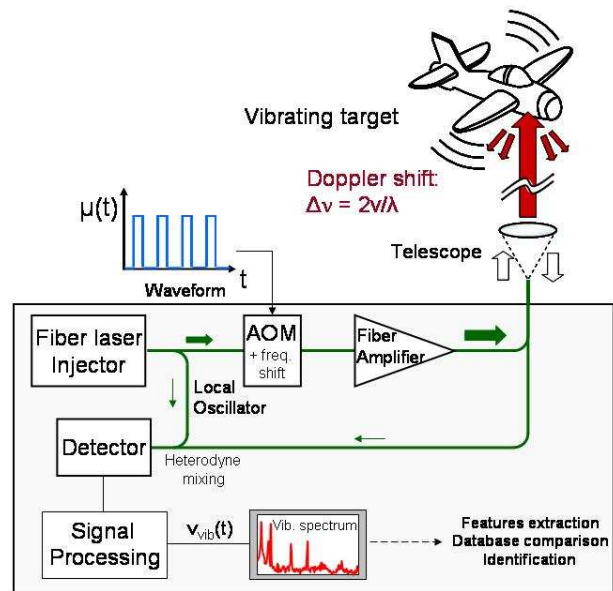

Figure 1. Diagram of a typical all-fiber vibrometer laser radar, for target identification applications. AOM : acousto-optic modulator, adding frequency shift f_{AOM}.

The performance of the measurement is often characterized in terms of how much these peaks stand out from the measurement noise floor on this spectrum (this is indicated by the Signal-to-Noise Ratio, SNR).

Ladar vibrometers with a pulsed emission usually use the acousto-optic modulator as an amplitude modulator to create pulsed waveforms (Fig. 1). At reception, each of them provides one velocity sample of the time series. A popular waveform inherited from meteorological radars is a basic pulse-pair [4], repeated as often as needed for the correct sampling of the vibration. The phase difference between pulses in a pair gives the

velocity estimate. More generally, pulsed laser radars benefit from radar expertise in waveform design and signal processing.

Several advantages of pulsed vibrometry have been highlighted [4]: the higher peak power allowed for the same mean laser power, the possibility of keeping a monostatic configuration even when aiming at fix targets, and the capability to perform simultaneous telemetry by measuring the time of flight of the pulses. A pulsed vibrometer could then have longer range and be a more compact and multi-functional instrument than a Continuous-Wave (CW) vibrometer.

Yet, pulsed mode has important drawbacks. Because of the fewer number of velocity measurements, it usually does not perform better, in terms of SNR, than CW mode. Amplitude and phase fluctuations are induced by the targeted surface movements (so-called speckle noise), by the laser linewidth and atmospheric turbulence. Pulsed mode has been shown to be particularly sensitive to such perturbations, as well as to independent vibrations of parts of the target under the laser beam [5]. Along with the compensation of the bulk Doppler shift caused by target global velocity, and the own vibrations of the ladar carrier platform, these problems are considered the main impediments to the use of pulsed vibrometry for the identification of vehicles.

In this paper, we propose advanced signal processing solutions to reduce the sensitivity of pulsed mode to measurement perturbations. We compare the performance of pulsed mode associated with these methods, to that of CW vibrometry, in harsh noise conditions. To remain independent of technological constraints, we consider an ideal emission in which a given mean laser power can be split into a number of pulses or emitted continuously. In addition to the classical pulse-pairs, we use poly-pulse waveforms [6], for their larger measurement dynamic.

After detailing the signal model adopted for this work, we recall some properties of poly-pulse waveforms in section 2. Section 3 reviews Instantaneous Frequency (IF) estimators that are already applied in CW vibrometry for the demodulation of the signal, or can be adapted to pulsed vibrometry. Then, in section 4, we propose and characterize a new Maximum Likelihood (ML) based IF estimator that takes into account noise statistics for better performance, as well as pseudo Time-Frequency Representations (TFRs) for pulsed mode, which allow noise regularization. Processing methods and operating modes (CW, pulse-pairs, poly-pulses) are compared in simulation in section 5. Section 6 concludes.

2. SIGNAL MODEL AND POLY-PULSE WAVEFORMS

The analytic signal, i.e. downshifted around null frequency, as can be obtained after I/Q demodulation, can be expressed as such:

$$i_S(t) = \mu(t).i_{het}(t) + i_b(t)$$
$$= \mu(t).i_0.m(t).\exp(j\varphi_{vib}(t)) + i_b(t) \quad (1)$$

where $\mu(t)$ is the amplitude modulation in pulsed mode ($\mu(t) = 1$ in CW mode), $i_{het}(t)$ is the heterodyne current, with a mean amplitude i_0, $m(t)$ is a complex multiplicative noise, circular and centered, with a variance normalized to 1, $\varphi_{vib}(t) = 4\pi.x_{vib}(t)/\lambda$ is the phase modulation caused by the targeted surface vibration displacement projected along the laser line of sight $x_{vib}(t)$ for the laser wavelength λ, and $i_b(t)$ is an additive complex noise (detector / photon noise), white, Gaussian valued, circular and centered, with variance σ_b^2. We will only deal with the relative strength of signal and noise by the means of the time averaged Carrier-to-Noise Ratio (CNR), defined as CNR = $<|i_{het}|^2> / <|i_b|^2> = i_0^2 / 2\sigma_b^2$.

Complex multiplicative noise $m(t)$ gathers amplitude and phase fluctuations terms, and is the result of several phenomena [7]:

- Target speckle noise is due to the movement and evolution of the speckle figure backscattered by the target as it moves, which varies the received optical wave. It is well described by a complex Gaussian variable with a Gaussian auto-correlation function $\Gamma(\tau) = \exp(-B_{speckle}^2\tau^2)$, where $B_{speckle}$ is the inverse of the correlation time, called speckle bandwidth. It can be up to several kilohertz.

- Laser phase noise is due to the spectral linewidth of the laser. As the optical path difference between measurement path and local oscillator path increases, so does the decorrelation between the two mixed waves, the result being a random phase term in m(t).

- The evolution of atmospheric turbulence in which the beam propagates produces amplitude and phase fluctuations.

Complex multiplicative noise impacts the measurement through signal fading as well as spectral broadening because of phase fluctuations, which directly affects the accuracy of the velocity estimation.

The signal model of Eq. 1 is based on several simplifying hypothesis: 1) it is assumed that any bulk Doppler shift due to target global velocity has previously been removed; 2) the sounded surface

vibrates as a whole, and there is no separate vibrators generating signals with various IFs; 3) we also suppose that we have previous knowledge of the target's distance, and know precisely which samples contain the signal (telemetry performed by the radar that was used to detect the target is sufficient for this); 4) we adopt the hypothesis of an equal mean laser power emitted for all operating modes, which implies taking $<\mu(t)^2> = 1$; 5) lastly, we neglect the phase effects of atmospheric turbulence and laser phase noise and only consider speckle noise. Laser phase noise can indeed be greatly reduced by using a well chosen delay line in the local oscillator path, and turbulence noise is negligible before speckle noise (unless the line of sight is low above the ground).

The speckle bandwidth is chosen of 5kHz, the same order of magnitude as the vibration induced signal bandwidth, considering cm/s peak-to-peak vibration velocities. CNR is given in the full sampling bandwidth of 1MHz. A common CNR value for all operating modes is obtained by using the mean signal power received instead of its peak value in pulsed mode.
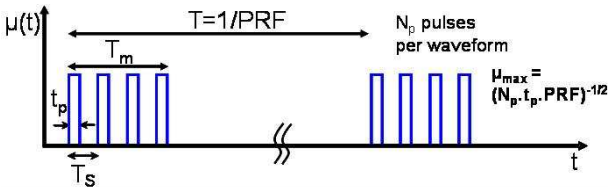

Figure 2. Characteristics of poly-pulse waveforms:

PRF: waveform repetition frequency, T_m: poly-pulse total duration, T_S: pulse time separation, t_p: pulse duration

Amplitude modulation $\mu(t)$ is formed of regular poly-pulses of square shape as described on Fig. 2. There are several main constraints on their parameters [6]: 1) waveform repetition frequency PRF must be properly chosen to respect Nyquist's criterion for the correct sampling of the vibration (PRF >2 $f_{vib,max}$, maximum vibration frequency); 2) in order to avoid velocity ambiguities, as the measured phase shift between pulses $\Delta\varphi = f_{inst}/(2\pi T_S)$ is only know within]- π; π] interval, pulse separation T_S must be shorter than $\lambda/4v_{max}$; 3) T_m must be short enough so that the IF remains roughly constant during the waveform ($T_m <<1/f_{vib,max}$), but as large as possible to allow a more accurate IF estimation (by Fourier's limit, IF is known with precision evolving as $1/T_m$).

As the same energy for all operating modes is split between pulses and $<\mu(t)^2> = 1$, the max value of $\mu(t)$ is $\mu_{max} = (N_p t_p PRF)^{-1/2}$. T_S being fixed by the expected maximum vibrational velocity of the target, the optimal number of pulses N_p may vary according to noise conditions [4]: in case the target is remote and the signal is weak, higher peak power should be preferred, and N_p be chosen

smaller. Pulse-pair is the limit of this trend, conceived to maximize peak power. On the contrary, if the signal is strong enough and complex multiplicative noise dominates, a larger number of measurements (and pulses) is preferable so as to average it out. An agile system would perform this adjustment; we will however consider the case of a fix number of pulses, chosen to allow a suitable measurement dynamic D, disregarding noise conditions:

$$D = V_{amb} / \delta V \qquad (2)$$

where:

$$V_{amb} = \lambda / (2\pi T_S) \qquad (3)$$

is the velocity ambiguity interval, and:

$$\delta V = \lambda / \left(8\pi \sqrt{\int t^2 \mu(t)dt} \right) \qquad (4)$$

is the velocity resolution. For instance, the dynamic of quadripulses is $D_{4p} \approx 28$ while the dynamic of pulse-pair is much smaller $D_{2p} \approx 9$. As is show in section 5, in conditions with strong complex multiplicative noise, poly-pulses perform much better than pulse-pairs, and remain as good in other cases unless the mean signal power is very weak and there is no phase noise.

Other waveforms are of course usable in this frame of work. For example, with staggered (irregular) poly-pulses with varying separations T_S, a good dynamic can be ensured by a smaller number of pulses, provided a large T_m and a small minimum separation between, for instance, the two first pulses. However, as the ambiguities that appear, with this type of waveform, are difficult to solve when dealing with bad noise conditions, we rather focused on regular poly-pulses.

3. IF ESTIMATION FOR COHERENT LASER RADAR VIBROMETRY

In this section, we recall the state of the art of signal processing for vibrometry by coherent laser radar. As introduced in section 1, the goal of the signal processing is to obtain the vibration velocity by IF estimation, and then determine the modal frequencies of vibration, whereas additive detection noise, and phase and amplitude noise disturb this estimation.

Three trends in literature from the laser radar, radar and signal processing domains, which apply to both CW and pulsed signals, are interesting to compare. The most computationally efficient, although the least robust to disturbances, is phase derivation over samples (CW) or pulses (pulsed), just as in conventional frequency demodulation.

A second trend relies on Time-Frequency processing, as introduced in vibrometry by Kachelmyer [8], with the spectrogram. This approach requires another step to obtain the vibration from the Time-Frequency Representation, by determining the frequency localization of the maximum of energy along time. The main advantages of this method, which remains much more costly in computation time, are a better overall performance than classical frequency demodulation, the possibility of following multiple traces generated by independent vibrations, and extracting them from noise using regularization techniques, as will be explained in section 4.

The third trend, parametric estimation of the peak vibration frequencies, would use the complete model of the signal (phase modulated by a sum of sinusoids), and directly adjust it to the data. This is theoretically the optimal processing given our signal model, but because of the non-stationarity of the vibrations and the usual deviations from the model, which have to be compensated by a large number of unknown parameters, it is not realistic to consider it for real-time processing. Therefore, it will not be studied in the current paper.

We now detail the estimators that will be implemented for each operating mode. In CW mode, three estimators are commonly used in literature. The first one is the centroid of the spectrogram columns [8], enhanced with a circular mean in order to avoid the bias due to the noisy background (SpectroGram Centroid, SGC):

$$\hat{f}_{inst}(t) = \frac{B}{2\pi} \arg\left(\int_B SG(t,f).\exp\left(j2\pi\frac{f}{B} \right) df \right) \quad (5)$$

where SG(t,f) is the spectrogram (square modulus of the short term Fourier transform) and B is the analysis bandwidth, usually matched to that occupied by the signal. Short term spectrum matching (Lee's Spectral Matching, LSM) [9] is also applicable on the columns of the spectrogram of the signal (as a maximum of correlation):

$$\hat{f}_{inst}(t) = \arg\max_f \left(S_{ref}(f) \otimes SG(t,f) \right) \quad (6)$$

where $S_{ref}(f)$ is a reference spectrum inferred thanks to the knowledge of $B_{speckle}$, which can be evaluated by studying the amplitude fluctuations of the signal. Lastly, the short term coherent average of the phase difference between consecutive samples (Autocorrelation First Lag, AFL) [5] is implemented by:

$$\hat{f}_{inst}(t) = \frac{1}{2\pi\Delta t} \arg\left(\sum_{n=1}^{N_m} i_s(t+n.\Delta t)i_s^*(t+(n-1).\Delta t) \right) \quad (7)$$

where Δt is the sampling period, and N_m the number of samples on which the short term autocorrelation is computed.

In pulsed mode, pulse-pairs are processed by the phase difference between pulses (Pulse-Pair, PP). Note that the precise time of arrival (i.e. target range) is supposedly known, which allows perfect temporal windowing:

$$\hat{f}_{inst}(t = k/PRF) = \frac{1}{2\pi T_S} \arg\left(<i_s>_{k,2} <i_s>_{k,1}^* \right) \quad (8)$$

where k, positive integer, is the number of the waveform et $<i_S>_{k,l}$ is the average of the signal over pulse #l of waveform #k.

With poly-pulses, we directly adapt the same principle by coherently averaging the phase difference over couples of consecutive pulses (Poly Pulse-Pair, PPP):

$$\hat{f}_{inst}(t = k/PRF) = \frac{1}{2\pi T_S} \arg\left(\sum_{l=2}^{N_p} <i_s>_{k,l} <i_s>_{k,l-1}^* \right) \quad (9)$$

with the same notations as in Eq. (5). Yet, it is rather advised [9,10] to estimate the phase rate also over non consecutive samples; this comes down to the linear regression of the phase of the received pulses autocorrelation function, i.e. the search of the maximum of their Fourier Transform (FT). This leads us to the second class of estimators presented before, which involves spectral analysis, the first one being simply based on the FT of the autocorrelation function (AutoCorrelation Fourier Transform, ACFT):

$$\hat{f}_{inst}(t = k/PRF) = $$
$$\arg\max_f \left(\left| \int \Gamma_{i_s,k}(\tau).h(\tau).\exp(-j2\pi f\tau)d\tau \right| \right) \quad (10)$$

where $\Gamma_{i_s,k}(\tau)$ is the autocorrelation function of waveform #k, and $h(\tau)$ is a window that is applied to select and balance the contribution of significant couples of pulses. We also implement the adapted filter frequency estimator of radars, which consists in finding the maximum of the spectrum of the received poly-pulse multiplied by the emitted one. (Poly Pulse Adapted Filter, PPAF):

$$\hat{f}_{inst}(t = k/PRF) = $$
$$\arg\max_f \left(\left| \int_{\text{Multiplet } k} i_s(t).\mu(t).\exp(-j2\pi ft)dt \right| \right) \quad (11)$$

in which the signal is restricted to poly-pulse #k. This estimator corresponds to the Maximum Likelihood (ML) estimator, in case of white additive noise.

4. ADVANCED SIGNAL PROCESSING METHODS

This last estimator is practical to process arbitrary waveforms, but it is not optimal in case anything else than a simple additive white noise affects the signal. That is why we propose to implement the

true ML estimator in the conditions of coherent laser radar.

Additional assumptions are made to reduce the free parameters in our model to the sole frequency of the signal: a stationary IF over duration T_m, and previous knowledge of noise parameters $B_{speckle}$ and CNR. For an easier implementation and faster computation, the likelihood expression uses a variable change introduced by Ghogho et al. [11]. The resulting Instantaneous Frequency Likelihood (IFL) estimator is:

$$\hat{f}_{inst}(t = k/PRF) = \underset{f}{\arg\max}\left(- \text{Re}(\vec{s}')^T.Q_{s'}^{-1}.\text{Re}(\vec{s}') - \text{Im}(\vec{s}')^T.Q_{s'}^{-1}.\text{Im}(\vec{s}')\right) \quad (12)$$

with $\vec{s}'$, vector with p^{th} element written as:

$$\vec{s}'(p) = <i_s>_{k,p} \exp(-j2\pi f.pT_S) \text{ for p} = 1,...,N_p \quad (13)$$

and:

$$Q_{s'} = CNR_{peak}Q_m + I_{N_p} \quad (14)$$

where Q_X designates the covariance matrix of variable X. $Q_{speckle}$ is thus the covariance matrix of the multiplicative noise, with element (p,q):

$$Q_m(p,q) = Q_{speckle}(p,q)$$
$$= \Gamma_{speckle}((p\text{-}q)T_S) = e^{-B_{speckle}^2 T_S^2 (p-q)^2} \text{ for p,q} = 1,...,N_p \quad (15)$$

IFL is the pulsed mode equivalent to Levin's ML estimator in CW laser radar. Like Levin's expression in the spectral domain, the likelihood expression used here quantifies how much, when the phase modulation of the signal due to an assumed IF is suppressed, the result is close to having the expected covariance matrix, given by the sum of the covariance matrices of multiplicative and additive noises. This estimator can also be seen as a Fourier Transform restrained to actually correlated pulses.

We have a few remarks about its use. As any ML estimator, IFL should obtain the best results in terms of SNR, but does not perform well in strong noise conditions or in case of deviations from the adopted signal model. Knowledge of parameters CNR and B_m, or an estimated $Q_{s'}$, is required; they can be evaluated by studying the amplitude of the signal. Also, IFL is adaptable to other forms of multiplicative noise than the simple speckle noise studied here, as long as the signal is still a Gaussian random variable: only the covariance matrix has to be adjusted accordingly.

Cramér-Rao Lower Bound calculations and velocity error simulations confirm the interest of IFL in case of strong speckle noise [12]. However, it remains that this ML based estimator is not expected to tolerate very important multiplicative or additive noise.

This is why we introduce another enhancement for pulsed vibrometry processing, which is based on the possibility of building a pseudo Time-Frequency Representation in this operating mode as well, for the three estimators we presented that rely on maximizing a function of frequency: PPS, CFT and IFL. Indeed, by stacking the functions to maximize horizontally, we obtain such pseudo TFRs, as seen for simulated signals on the left side of Fig. 4.
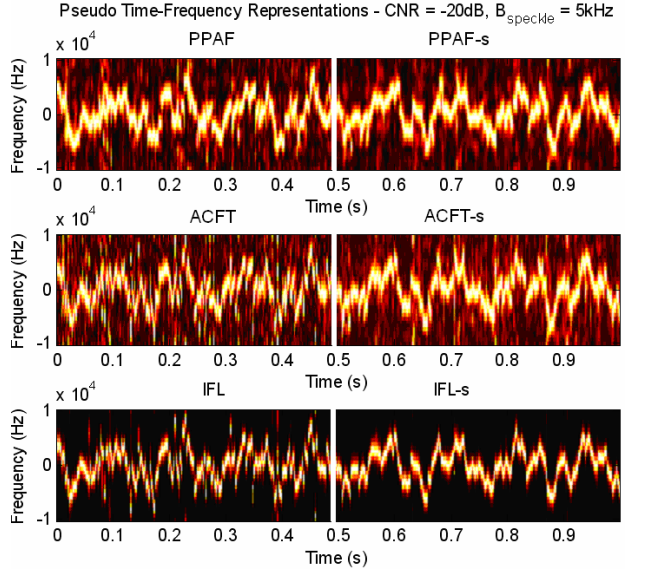

Figure 4. Pseudo TFRs obtained for simulated signals (6-pulse waveforms) with PPAF, ACFT, and IFL estimators, at low CNR. On the right side, temporal smoothing brings out the vibration trace.

On this pseudo TFR, extraction techniques can be applied that will take advantage of the continuity of the signal trace to better extract the vibration, and obtain higher SNR. We will merely indicate the potential of this noise regularization on the TFR by performing a simple temporal smoothing, the result of which is seen on the right side of Fig. 4. In section 5, the estimators that beneficiate of temporal smoothing are noted with suffix –s.

Pseudo TFRs in pulsed mode will allow the same possibilities that are already available in CW mode for noise regularization, as shown here, but also for better robustness in the case of multiple independent vibrations of parts of the target. Advanced extraction techniques remain to be developed, although centroiding is already a suitable tool, which will be used here.

5. COMPARATIVE SIMULATIONS

We now study the performance of the advanced processing methods introduced in section 4, relative to the existing estimators of section 3. The comparison is conducted on simulated signals as defined in the model detailed in section 2. Performance is calculated in terms of SNR on the

vibration spectrum, as the ratio of Power Spectral Density (PSD) at the modal frequency over the PSD of the noise floor.

The simulated vibration consists of 5 modes between 8 and 120 Hz, with 5mm/s peak vibration velocity. The given SNR values are the average of the 5 individual SNRs, over 200 realisations of the signal. The parameters of the waveforms are $t_p = 2\mu s$, $T_S = 50\mu s$. The waveform repetition frequency is chosen a little above Nyquist's criterion: PRF = 500Hz. CNR is measured as the mean CNR in a 1MHz bandwidth. $B_{speckle}$ is 5kHz. The analysis bandwidth B is fixed by $1/T_S$ at 20kHz.
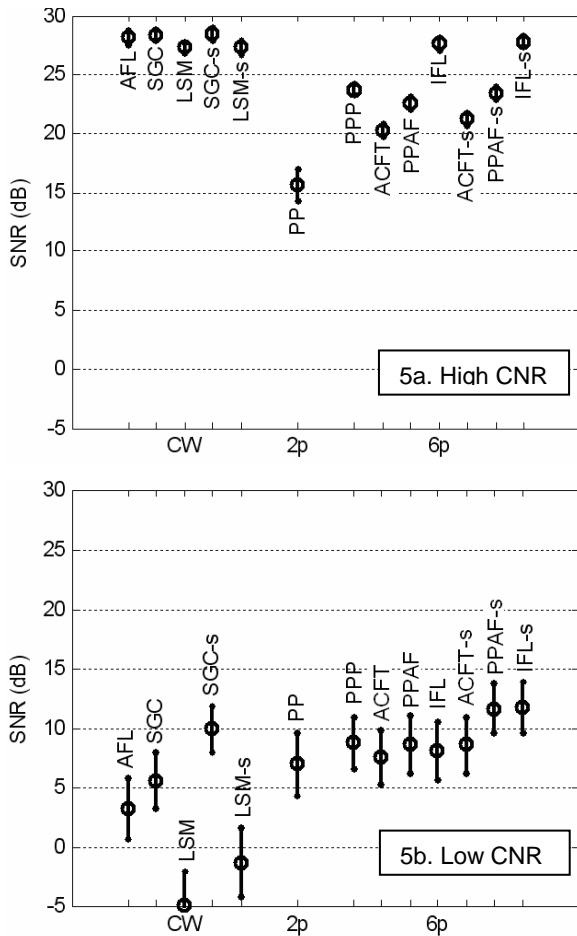

Figure 5a (top) and 5b (bottom). Average SNRs obtained at $B_{speckle}$ = 5 kHz and a) high CNR (30dB) or b) low CNR (-25dB). 2p = pulse-pairs. 6p = 6-pulse waveforms. Report to section 3 and 4 for estimator acronyms.

Fig. 5a gives the results obtained at high CNR for the various operating modes, when the effects of speckle noise are dominant. SNR results confirm the advantage of IFL over all other processing methods in pulsed vibrometry when speckle noise is dominant. In particular, there is a 5dB gain over standard radar processing PPAF. Pulse-pair operation is affected the most, more than 10dB below the best results obtained with 6-pulse

waveforms. We note that PPP processing obtains good results for a very short computation time.

At very low CNR (-25dB), as seen on Fig. 5b, as expected, pulsed mode obtains higher SNR. High peak power waveforms like pulse-pair should then be better than 6-pulse waveforms, but because speckle noise is strong, the latter are preferable. In CW mode, SGC allows the best SNR, while LSM is badly affected by strong detection noise. With poly-pulse waveforms, all estimators are roughly equivalent. Temporal smoothing benefits more to SGC processing in CW (5dB gain) than to IFL and PPAF processing with poly-pulses (3dB gain). This is because of the lesser number of averaged columns of the pseudo RTF in pulsed mode. We also note that IFL and PPAF are equivalent when the effects of speckle noise are not predominant.

We conduct another performance simulation with a varying analysis bandwidth B, that was previously fixed at 20kHz to match the vibration bandwidth. This assumption was in fact very restrictive because, in practice, the bandwidth of the vibration is unknown, so T_S and thus $B = 1/T_S$ have to be chosen large enough so that no velocity ambiguity is possible. So the bandwidth ratio $\alpha = B/B_{vib}$ may vary. On Fig. 6, we plot average SNR as function of α, at a low CNR (-20dB).
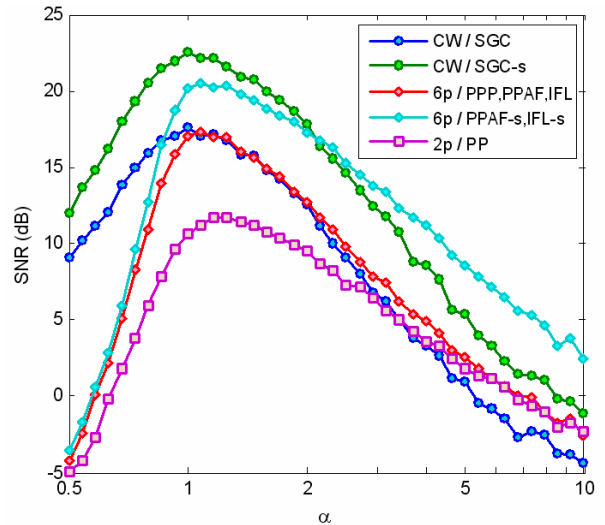

Figure 6. Average SNRs plotted as a function of α ratio between analysis bandwidth B and vibration bandwidth B_{vib}. 2p = pulse-pairs. 6p = 6-pulse waveforms. Report to section 3 and 4 for estimator acronyms.

It shows that SNR is very dependent of the analysis bandwidth. When $\alpha < 1$, as expected, signals losses and Doppler ambiguities deteriorate the measurement, especially in pulsed mode. For $\alpha > 1$, the various estimators react differently to the larger noise accepted in the analysis bandwidth. Temporal smoothing in both CW and pulsed mode is necessary to avoid a fall of SNR beyond $\alpha = 2$. For instance, for a 100kHz analysis bandwidth, i.e. $T_S = 10\mu s$ and $\alpha = 5$, only pulsed mode with poly-

pulse waveforms processed by IFL or PPAF and pseudo TFR temporal smoothing is able to retain around 10dB SNR. In some conditions, even with strong speckle noise, pulsed mode as enhanced by the methods described in this article can be preferable, because of its robustness to additive noise.

Other parameters, such as waveform repetition frequency PRF, have an important impact on the final SNR. Simulations show that optimal PRF in the given noise conditions is 1500Hz, because averaging numerous velocity measurements is more important in that case than having independently precise ones. A comprehensive study would also include the effects of noise and vibration parameters.

6. CONCLUSION AND FUTURE WORKS

In this paper, we have presented and compared common and advanced signal processing techniques applicable to pulsed laser vibrometry. The aim was to enhance the SNR on the measured vibration spectrum, in the case when the measurement is made difficult by strong speckle noise. It has indeed been shown before that speckle noise can reduce the interest of pulsed vibrometry, compared to CW vibrometry, which averages numerous velocity measurements.

In the hypothesis the mean output power of the laser is the main limitation, poly-pulse waveforms do not present as much peak CNR gain at long range than pulse-pairs, but allow better measurement dynamic, and are more robust to the said noise conditions. For these waveforms, we introduced specific processing based on Maximum Likelihood estimation, which takes into account the noise statistics and allows optimal velocity precision, as shown by a comparison with the theoretical precision limits (Cramér-Rao Lower Bound). Also, we proposed to build pseudo Time-Frequency Representations for estimators based on spectral analysis in pulsed mode. They open interesting possibilities for noise regularization.

The global comparison of the simulated SNR performance of all presented methods, for vibrometry with CW, pulse-pair and 6-pulse waveforms, shows that poly-pulse waveforms with our Instantaneous Frequency Likelihood processing obtains the best results at high CNR. Also, at low CNR, a simple temporal smoothing of the pseudo TFR was proven very beneficial. With the said enhancements, pulsed vibrometry remains preferable at low CNR, with a realistically large analysis bandwidth, despite the large speckle noise considered in all this study.

Present and future works include the confirmation of these results in a laboratory experiment, the development of techniques to better extract the vibration from a TFR, while remaining robust to independent vibrations of parts of the target, and an optimization study of waveforms and signal processing for pulsed vibrometry considering the actual limitations of fiber lasers.

7. REFERENCES

1. Guéguen, P., Jolivet, V., Michel C. et al (2009). Comparison of velocimeter and coherent LIDAR measurements for building frequency assessment. *Bulletin of Earthquake Engineering*, in press.

2. Kranz, W. (1989). Target Classification by Laser Vibration Sensing, *Proc. of SPIE* **1181**, 301-306

3. Lutzmann, P., Frank, R., Hebel, M. et al (2004). Potential of Remote Laser Vibration Sensing for Military Applications. *RTO SCI Symposium, Brussels*

4. Hannon, S.M., Thomson J.A., Henderson S.W. et al (1998). Agile Multiple Pulse Coherent Lidar for Range and Micro-Doppler Measurement, *Proc. of SPIE* **3380**, 259-269

5. Hill, C., Harris, M., Ridley, K.D. et al (2007). Fiber-based 1.5 µm lidar vibrometer in pulsed and continuous modes. *Applied Optics* **46**, 4376-4385

6. Gatt, P., Henderson, S.W., Krause, B. (2006). Poly-pulse Coherent Lidar Waveforms for Coherent Lidar Measurements, *Coherent Optical Technologies and Applications Conference, Whistler, Canada*

7. Gatt, P., Henderson, S.W., Thomson, J.A. et al (2000). Noise Mechanisms Impacting Micro-Doppler Lidar Signals: Theory and Experiment, *Coherent Technologies, Inc. Technical Report*

8. Kachelmyer, A.L. and Schultz, K.I. (1993) Spectrogram Processing of Laser Vibration Data, *Proc. of SPIE* **1936**, 78-88

9. Youmans, D. G. (2005). Target Spectral Estimation using Direct Detection and Coherent Detection Ladar, *Proc. of SPIE* **5791**, 97-108

10. Rye, B. J. and Hardesty, R. M. (1993). Discrete Spectral Peak Estimation in Incoherent Backscatter Heterodyne Lidar, *IEEE Trans. on Geoscience and Remote Sensing* **31**, 16-35

11. Ghogho, M., Nandi, A. K., Swami, A. (2001). Cramér-Rao Bounds and Maximum Likelihood Estimation for Random Amplitude Phase-Modulated Signals, *IEEE Trans. on Signal Processing* **49**, 2905-2916

12. Totems, J., Jolivet, V., Ovarlez, J.P. et al. (2009). Signal Processing Methods and Poly-Pulse Waveforms for Laser Vibrometry in Pulsed Mode, *15th Coherent Laser Radar Conference, Toulouse*